한국가시화정보학회지, 제5권, 제1호, (2007) 3~8
<특집기사>

모세관 리소그라피를 이용한 고종횡비 나노구조 형성법

정훈의* · 이성훈* · 김필남* · 서갑양†

Capillary-driven Rigiflex Lithography for Fabricating High Aspect-Ratio Polymer Nanostructures

Hoon Eui Jeong, Sung Hoon Lee, Pilnam Kim and Kahp Y. Suh

Abstract. We present simple methods for fabricating high aspect-ratio polymer nanostructures on a solid substrate by rigiflex lithography with tailored capillarity and adhesive force. In the first method, a thin, thermoplastic polymer film was prepared by spin coating on a substrate and the temperature was raised above the polymer's glass transition temperature (T_g) while in conformal contact with a poly(urethane acrylate) (PUA) mold having nano-cavities. Consequently, capillarity forces the polymer film to rise into the void space of the mold, resulting in nanostructures with an aspect ratio of ~ 4. In the second method, very high aspect-ratio (>20) nanohairs were fabricated by elongating the pre-formed nanostructures upon removal of the mold with the aid of tailored capillarity and adhesive force at the mold/polymer interface. Finally, these two methods were further used to fabricate micro/nano hierarchical structures by sequential application of the molding process for mimicking nature's functional surfaces such as a lotus leaf and gecko foot hairs.

Key Words: Nano patterning(나노패터닝), Capillarity(모세관현상), Adhesive force(접착력), High aspect ratio(고종횡비), Nanohairs(나노섬모)

1. Introduction

Fabrication of high aspect-ratio (AR) nanostructures has attracted much attention due to its wide range of applications such in sensor arrays[1], high capacitance in DRAM[2], field emitters[3], biological studies[4] and biomimetics[5-7]. In spite of increasing demand, high AR nanostructures are difficult to fabricate by conventional photolithography or electron-beam lithography because high AR structures are prone to collapse during developing. Typical microelectromechanical processes such as LIGA and deep reactive ion etching (DRIE) are also difficult to use due to their inherent limitations for the sub-100-nm patterning[8].

Unconventional contact-based methods (e.g., nanoimprint[9] or soft lithography[10]) have been suggested as an alternative for fabricating high AR structures. These techniques are relatively simple and economically viable, offering a low-expertise route to many polymeric micro/nanostructures. However, some limitations prevent the widespread use of these techniques. For example, nanoimprint lithography could not be directly applied to the fabrication of high AR structures due to the rigidity of the mold (Young's modulus > ~100 GPa) and the limited film thickness. For soft lithography, polydimethylsiloxane (PDMS) mold is widely used for its favorable optical property and facile processibility. The potential limitation is that PDMS mold is difficult to be used for fabricating high aspect-ratio sub-100-nm structures due to its low Young's modulus (~ 1.8 MPa)[11,12].

Recently, a UV-curable polyurethane acrylate (PUA) mold was introduced for fabricating high AR nanostructures[13]. Since PUA mold is suffi-

†서울대학교 기계항공공학부
E-mail: sky4u@snu.ac.kr
*서울대학교 기계항공공학부

ciently rigid (Young's modulus of ~ 40 MPa) for the sub-100-nm patterning, yet it is also flexible (~ 50 μm thickness), it can make an intimate contact with the substrate over a large area, combining major advantages of imprint and soft lithographies (so called "rigiflex lithography")[14].

Here, we present various capillary-driven rigiflex lithographic methods for fabricating high AR polymeric nanostructures. With the aid of flexibility and rigidity of the PUA mold, high AR (~ 4) nanostructures can be easily obtained on a large area. Moreover, simple modifications of the mold material can give rise to elongation of the preformed nanostructures, resulting in very high AR (> 20) nanohairs upon removal of the mold. We further endeavor to test these methods for fabricating micro/nano hierarchical structures by sequential application of the molding process. Such a sequential process leads to a dense nanostructure on top of the pre-formed microstructure, which is reminiscent of nature's functional surfaces such as a lotus leaf and gecko foot hairs.

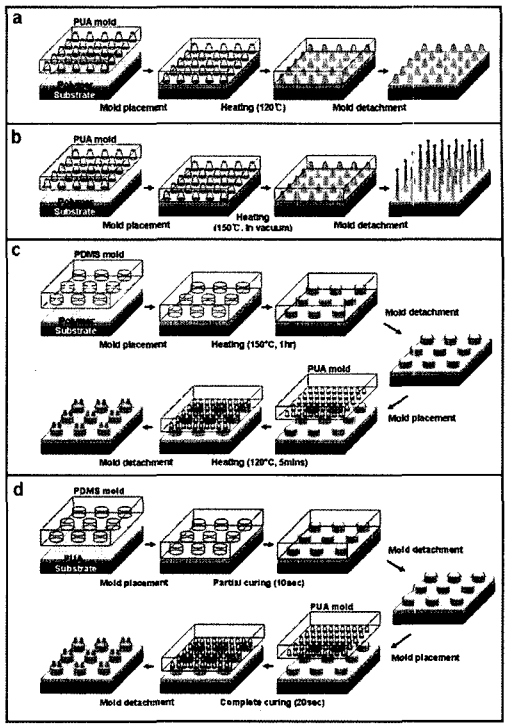

Fig. 1. Schematic drawings of the four different molding processes used in the experiment.

2. Meterials and Methods

For fabricating polymer nanostructures (figure 1a), silicon wafer was cleaned by ultrasonic treatment in trichloroethylene and methanol for 5 min each and dried in nitrogen. For the polymer, we used commercial poly(methylmethacrylate) (PMMA) (M_w=1.2×10^5, T_g=105°C, Aldrich) dissolved in toluene (10 wt%). The PMMA polymer was spin-coated onto the silicon substrate and the PUA mold (surface tension ~ 12.3 mJ/m^2) was placed on the polymer surface under a slight pressure (~10 g/cm^2) for conformal contact with the polymer. For a uniform pressure distribution, a thin PDMS block was placed as a buffer on top of the PUA mold prior to the application of pressure. Then the sample was annealed at 120°C, well above the glass transition temperature for 30 min on a hot stage.

For fabricating high aspect-ratio polymer nanostructures (figure 1b), the PUA mold with higher surface energy (surface tension ~ 30.8 mJ/m^2) was placed on the polymer surface under a slight pressure (~10 g/cm^2) to make conformal contact and the temperature was raised above T_g (typically at 150°C) for >1 hr. Then the polymer rises into the mold's cavities by capillary action. The subsequent removal of the PUA mold stretches the nanostructures, resulting in high AR, stretched nanohairs (AR > 20) over a large area[15].

For fabricating multiscale hierarchical structures, two different methods were used. In the first method (figure 1c), a patterned PDMS mold was placed onto the spin-coated PMMA surface on the silicon substrate. Then the sample was annealed at 150°C for 1 hr on a hot stage. After fabricating a microstructure, the PUA mold was placed on the as-prepared microstructure under a slight pressure (~10 g/cm^2) for conformal contact with the polymer. Then the polymer was annealed again at 120 °C for 5 min on a hot stage to fabricate nanostructures[16].

In the second method (figure 1d), a patterned PDMS mold was placed onto the spin-coated, UV-curable PUA resin on the silicon substrate. Then the PUA resin was partially cured by UV exposure for 10 sec (λ = 250 ~ 400 nm, dose = 100 mJ/cm^2). After fabricating a partially cured microstructure,

the PUA mold was placed on the as-prepared microstructure followed by additional UV exposure for 20 sec to fabricate nanostructures with the completion of curing of the PUA resin.

3. Results

Figure 1 shows schematic drawings of the four different molding processes used in the experiment. For simple capillary-driven molding process (figure 1a), a negative PUA mold (features sticking in) had been replicated by exposing the uncured PUA to UV[13]. The uncured PUA was poured on the complementary Si master prior to the UV exposure. A thin sheet-type (~50 mm) PUA mold can make conformal contact with a low pressure (~10 g/cm^2) as compared to nanoimprint lithography[9] and expel the trapped air easily at the time of contact, enabling a large area patterning. For nanodrawing process (figure 1b), the adhesive force between the mold and the polymer was tailored such that the filled nanostructures was further elongated upon removal of the mold. Finally, the methods were used to obtain a hierarchical structure by sequential application of the rigiflex lithography (figure 1c-d). For this purpose, a micropatterned PDMS mold was first used for fabricating microstructures and then a nanopatterned PUA mold was applied for nanostructures. The resulting structures can either be simply replicated nanostructures on the pre-formed microstructures or stretched nanohairs on the same micropattern.

Figure 2a shows a scanning electron microscopy (SEM) image of the precisely patterned PMMA nanopillars. The AR of the nanopillars is ~4 with ~150 nm width and ~ 600 nm height, suggesting that the polymer reaches the ceiling of the mold with height of 600 nm. The key factor for complete capillary rise lies in removing the trapped air carefully[17]. If the mold makes a contact with the polymer surface from the edge, the air could be trapped, inhibiting capillary rise somewhere in the cavity. In this case, the maximum capillary rise is determined by balancing capillary force and hydrodynamic pressured built up in the cavity as the capillarity proceeds. In our experiment, the mold was brought in contact from one edge to the other, thereby minimizing the effects of the trapped air.

To further increase the AR of nanostructures for a given mold geometry, nanodrawing process aided by modulated interfacial tensions was used as shown in figure 2b-c. When the cavities of a mold are filled with a polymer having a relatively high adhesion (not too high) to the mold, the filled polymer structure can be elongated to form very long, stretched polymer nanohairs, which can be viewed as an intermediate process between simple replication (figure 1a) and detachment[18-20]. If the adhesive forces between the mold/polymer interface and the polymer/substrate interface are comparable, high AR nanostructures result instead of simply replicated or delaminated structures. This condition is given by

$$r = \frac{W_{23} \cdot A_{23}}{W_{12} \cdot A_{12}} \cong 1 \qquad (1)$$

where $W_{12(23)}$ and $A_{12(23)}$ are the work of adhesion and surface area at the polymer/substrate (mold/polymer) interface, respectively.

Figure 2b-c shows SEM images of the stretched poly(methyl methacrylate) (PMMA) nanohairs. The height of the nanohairs ranged from 1.5 to 2 mm and the diameter was ~ 80 nm, rendering an AR larger than 20.

For the nanodrawing process, the adhesion energy ratio needs to be optimized around 1. Furthermore, the drawing temperature is also important. Even with an optimum value of the adhesion energy ratio (r ~ 1), polymer film was found to delaminate from the substrate or fracture at the middle or base of the nanostructure if the temperature was lower than ~ 90°C, which is attributed to extremely high mechanical modulus and viscosity below T_g. Hence, the drawing needs to be carried out above 90°C for uniform elongation of the nanostructures without fracture[15].

The above-mentioned methods can also create a hierarchical structure by applying rigiflex lithography in a sequential manner (figure 1c-d). Hierarchical structures seem ubiquitous in nature's functional surfaces for adapting to any surface roughness and mechanical stability[21-24]. The fabrication proceeds in two steps: (i) the fabrication of polymer microstructures using a low-resolution, micropatterned PDMS mold and (ii) subsequent nanofabrication using a high-resolution nanopatterned PUA mold

on top of the pre-formed polymer microstructures. Figure 2d shows an SEM image of the hierarchical structure consisting of microposts with nanoscale pillars fabricated by the two-step temperature-directed molding process. In this method, the pre-formed microstructure is prone to collapse above T_g in the presence of a small mechanical loading. Thus, the heating time should be controlled below 20 min to minimize substantial deformation of the preformed microstructure[16].

To overcome this limitation, we prevent here an improved version of the two-step molding process, which utilizes UV-curable resins (e.g. PUA) instead of thermoplastic polymers. Figure 2e-f shows SEM images of hierarchical structures consisting of nanolines or nanopillars on top of the pre-formed microstructures. In this case, nanostructures were precisely formed without any collapse or deformation of the predefined microstructure within 1 min. It was found that the UV-curing time for the partial curing of microstructure was a crucial factor. If the curing time is too short, the microstructure was easily collapsed. If the time is too long, on the other hand, the nanostructures can not be formed on the completely cured microstructure due to non-fluidity of the PUA resin.

The high AR nanostructures (figure 2b-c) and multiscale hierarchical structures (figure 2d-f) presented here are potentially useful for studying nature's functional surfaces. Typical examples are the surface of a lotus leaf and gecko foot hairs. It was revealed that micro/nanoscale hierarchical structures on the surface of a lotus leaf further increases the contact angle of water and reduces the sliding angle or the difference between advancing and receding contact angles[23]. The superhydrophobicity on the surface with complex hierarchical structures has already been demonstrated either by using a top-down or a bottom-up approach[25-31].

Another example is the gecko foot with an extremely high AR. The gecko foot structures are hierarchical such that threefold length scales exist from millimeters, micrometers, to nanometers (figure 3a)[24]. These multi-scaled structures can make it possible for the gecko to adapt to any surface roughness, allowing for a highly efficient, natural dry adhesive. In contrast, the stretched nanohairs presented in this study consist of single scale nanohairs and thus the adhesion ability would be much decreased.

To fabricate a flexible gecko tape, a PET film (50 μm in thickness) was attached to the sticky surface of a commercially available 3M tape. The subsequent procedure was the same after spin coating of a PMMA solution onto the non-sticky tape surface. Figure 3b shows an example of the flexible tape prepared by the nanodrawing method. On the surface, dense nanohairs were fabricated over a large area without many defects (figure 3c). An actual adhesion test shown in Figure 3d revealed

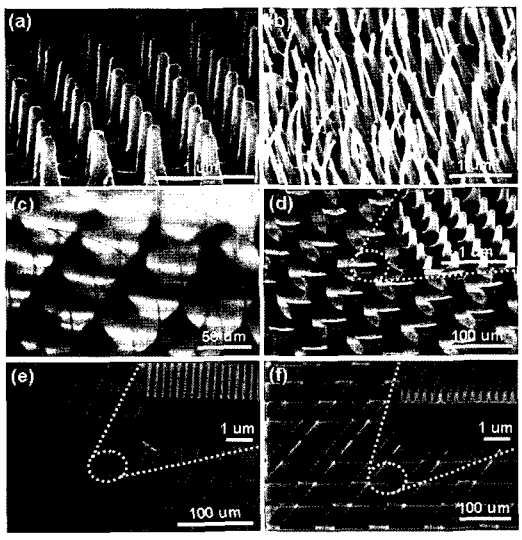

Fig. 2. Examples of the fabricated nanostructures.

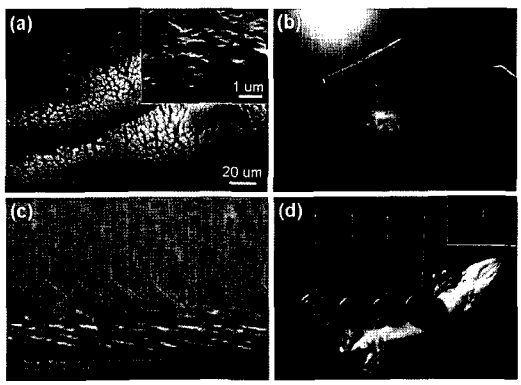

Fig. 3. (a) SEM image of real gecko foot hair structures. (b-d) An example of the fabricated flexible gecko tape.

that the maximum load was 3~4 N/cm^2, several times lower than the theoretically estimated value based on the adhesion force of a single nanohair and the density of the nanohair (~ 7 N/cm^2). This value is approximately one order of magnitude smaller than the maximum adhesion of the gecko (~ 10 N/cm^2)[32]. The use of a softer material with hierarchical dimensions would further enhance the adhesion performance of the current tape.

4. Discussion

We have presented the fabrication of high aspect-ratio nanostructures by rigiflex lithography with tailored capillarity and adhesive force. It was found that high AR polymer nanostructures (>20) and micro/nanoscale hierarchical structures could be fabricated with high-resolution PUA mold. It is hoped that this method could provide a versatile, economically viable route to fabrication of high AR nanostructures for mimicking various bio-inspired functional surfaces.

Acknowledgements

This work was supported by the Korea Institute of Machinery & Materials (KIMM).

References

1) Aimi, M.F., Rao, M.P., Macdonald, N.C., Zuruzi, A.S. and Bothman, D.P., 2004, "High-aspect-ratio bulk micromachining of titanium," Nature Materials, Vol.3(2), pp.103-105.
2) Jang, J.E. et al., 2005, "Nanoscale capacitors based on metal-insulator-carbon nanotube-metal structures," Appl. Phys. Lett., Vol.87(26), -.
3) Rangelow, I.W. and Biehl, S., 2001, "Fabrication and electrical characterization of high aspect ratio silicon field emitter arrays," J. Vac. Sci. Technol. B, Vol.19(3), pp.916-919.
4) Tan, J.L. et al., 2003, "Cells lying on a bed of microneedles: An approach to isolate mechanical force," P. Natl. Acad. Sci. USA, Vol.100(4), pp. 1484-1489.
5) Geim, A.K. et al., 2003, "Microfabricated adhesive mimicking gecko foot-hair," Nature Materials, Vol. 2(7), pp.461-463.
6) Sitti, M. and Fearing, R.S., 2003, "Synthetic gecko foot-hair micro/nano-structures as dry adhesives," J. Adhesion Science and Technology, Vol.17(8), pp. 1055-1073.
7) Yurdumakan, B., Raravikar, N.R., Ajayan, P.M. and Dhinojwala, A., 2005, "Synthetic gecko foot-hairs from multiwalled carbon nanotubes," Chemcal Communications Vol.(30), pp.3799-3801.
8) Madou, M.J., 2002, "Fundamentals of microfabrication : the science of miniaturization," CRC Press, Boca Raton, Fla.
9) Chou, S.Y., Krauss, P.R. and Renstrom, P.J., 1996, "Imprint lithography with 25-nanometer resolution," Science, Vol.272(5258), pp.85-87.
10) Xia, Y.N. and Whitesides, G.M., 1998, "Soft lithography," Annu. Rev. Mater. Sci., Vol.28, pp.153-184.
11) Hui, C.Y., Jagota, A., Lin, Y.Y. and Kramer, E.J., 2002, "Constraints on microcontact printing imposed by stamp deformation," Langmuir, Vol.18(4), pp.1394-1407.
12) Bietsch, A. and Michel, B., 2000, "Conformal contact and pattern stability of stamps used for soft lithography," J. Appl. Phys., Vol.88(7), pp.4310-4318.
13) Choi, S.J., Yoo, P.J., Baek, S.J., Kim, T.W. and Lee, H.H., 2004, "An ultraviolet-curable mold for sub-100-nm lithography," J. Am. Chem. Soc., Vol.126 (25), pp.7744-7745.
14) Suh, D., Choi, S.J. and Lee, H.H., 2005, "Rigiflex lithography for nanostructure transfer," Adv. Mater., Vol.17(12), pp.1554-1560.
15) Jeong, H. E., Lee, S. H., Kim, P., Suh, K. Y., 2006, "Stretched polymer nanohairs by nanodrawing," Nano. Lett., Vol.6, pp.1508-1513.
16) Jeong, H. E., Lee, S. H., Kim, J. K., Suh, K. Y., 2006, "Nanoengineered multiscale hierarchical structures with tailored wetting properties," Langmuir Vol.22, pp.1640-1645.
17) Suh, K.Y., Choi, S.J., Baek, S.J., Kim, T.W. and Langer, R., 2005, "Observation of high aspect ratio nanostructures using capillary lithography," Adv. Mater., Vol.17, pp.560-564.
18) Stutzmann, N., Tervoort, T.A., Bastiaansen, K. and Smith, P., 2000, "Patterning of polymer-supported metal films by microcutting," Nature, Vol.407 (6804), pp.613-616.
19) Kim, C., Burrows, P.E. and Forrest, S.R., 2000, "Micropatterning of organic electronic devices by cold-welding," Science, Vol.288(5467), pp.831-833.
20) Choi, J.H., Kim, D., Yoo, P.J. and Lee, H.H., 2005, "Simple detachment patterning of organic layers and its application to organic light-emitting diodes," Adv. Mater., Vol.17(2), p.166-+.
21) Neinhuis, C. and Barthlott, W., 1997, "Characterization and distribution of water-repellent, self-cleaning plant surfaces," Ann. Bot-London, Vol.79(6), pp. 667-677.
22) Ball, P., 1999, "Engineering - Shark skin and other solutions," Nature, Vol.400(6744), p.507-+.
23) Feng, L. et al., 2002, "Super-hydrophobic surfaces: From natural to artificial," Adv. Mater., Vol.14(24),

pp.1857-1860.

24) Arzt, E., Gorb, S. and Spolenak, R., 2003, "From micro to nano contacts in biological attachment devices," P. Natl. Acad. Sci. USA, Vol.100(19), pp. 10603-10606.

25) Zhao, N. et al., 2005, "Fabrication of biomimetic superhydrophobic coating with a micro-nano-binary structure," Macromol. Rapid. Comm., Vol.26(13), pp.1075-1080.

26) Erbil, H.Y., Demirel, A.L., Avci, Y. and Mert, O., 2003, "Transformation of a simple plastic into a superhydrophobic surface," Science, Vol.299(5611), pp. 1377-1380.

27) Lu, X.Y., Zhang, C.C. and Han, Y.C., 2004, "Low-density polyethylene superhydrophobic surface by control of its crystallization behavior," Macromol. Rapid. Comm., Vol.25(18), pp.1606-1610.

28) Xie, Q.D. et al., 2004, "Facile creation of a bionic super-hydrophobic block copolymer surface," Adv. Mater., Vol.16(20), p.1830-+.

29) Thangawng, A.L. and Lee, J., 2004, "Fabrication of micro/nano integrated roughened structure using nanosphere lithography (NSL)," 2004 ASME International Mechanical Engineering Congress. Proceedings of IMECE04, Anaheim, pp. 13-20.

30) Li, S.H. et al., 2002, "Super-hydrophobicity of large-area honeycomb-like aligned carbon nanotubes," J. Phys. Chem. B, Vol.106(36), pp.9274-9276.

31) Lau, K.K.S. et al., 2003, "Superhydrophobic carbon nanotube forests," Nano. Lett., Vol.3(12), pp.1701-1705.

32) Autumn, K. et al., 2000, "Adhesive force of a single gecko foot-hair," Nature, Vol.405(6787), pp.681-685.